

## Original research

# Bacterial Diversity in Oil Field Environments and Evaluation of Their Ability to Biosynthesize Silver Nanoparticles (AgNPs)

Alaa H. Hamel<sup>1</sup>, Wijdan H. Al-Tamimi<sup>2†</sup> and Murtadha H. Fayadh<sup>1</sup>

<sup>1</sup>Department of Biology, College of Education for Pure Sciences, University of Basrah, Basrah 61004, Iraq

<sup>2</sup>Department of Biology, College of Science, University of Basrah, Basrah 61004, Iraq

†Corresponding author: Wijdan H. Al-Tamimi. wijdan.abdulsahib@uobasrah.edu.iq

<sup>2</sup>ORCID IDs of Authors: 0000-0002-5474-334X

Key Words	Oil environments, Universal 16SrDNA gene, Silver nanoparticles synthesis
DOI	<a href="https://doi.org/10.46488/NEPT.2026.v25i01.D1801">https://doi.org/10.46488/NEPT.2026.v25i01.D1801</a> (DOI will be active only after the final publication of the paper)
Citation for the Paper	Hamel, A.H., Al-Tamimi, W.H. and Fayadh, M.H., 2026. Bacterial diversity in oil field environments and evaluation of their ability to biosynthesize silver nanoparticles (AgNPs). <i>Nature Environment and Pollution Technology</i> , 25(1), p. D1801. <a href="https://doi.org/10.46488/NEPT.2026.v25i01.D1801">https://doi.org/10.46488/NEPT.2026.v25i01.D1801</a>

## ABSTRACT

Bacteria isolated from oil reservoirs environment possess unique enzymes that allow them to adapt to extreme environments, making them ideal candidates for producing high-value nanomaterials that can be used in various fields. In the present study, eight samples were collected from Badra and Ahdab oil fields in Iraq, the bacteria isolated and identified based on the *16SrDNA* gene, the isolates were screened for the synthesis of silver nanoparticles (AgNPs). The characteristics of the AgNPs were analyzed using UV-Vis spectroscopy, FTIR, XRD, FE-SEM, zeta potential measurements, and dynamic light scattering (DLS). The results indicated the dominance of Gram-positive bacteria, with percentage 18 (72%). Genetic identification revealed that bacteria was under 6 genera and 16 species, these genera include, *Enterococcus*, *Prieschia*, *Enterobacter*, *Acinetobacter*, *Flavobacterium*, and *Bacillus*. Seven new strains have been deposited in GenBank. The results of screening isolates for synthesized AgNPs showed high efficiency of a novel strain, *Bacillus halotolerans* strain AhWM4, with the maximum absorption peak at 430 nm. The average size of AgNPs using XRD, FE-SEM, and TEM was (31.3, 27.0, and 42.1) nm, respectively, dynamic light scattering (DLS) measurements showed a wide dispersion with an effective diameter of 57.1 nm, the X-ray diffraction (XRD) spectrum matched the crystalline nature of the AgNPs. It also showed high stability, with a zeta potential of -42.3 mV. AgNPs have attracted considerable attention due to their staggering potential for a wide range of commercial and environmental applications.

## INTRODUCTION

The biosynthesis of silver nanoparticles (AgNPs) has been explored in various environments, but using bacteria isolated from harsh conditions such as oil reservoirs characterized by the lack of oxygen, high temperatures, and extreme pressures represents a significant innovation. These extreme environments challenge most forms of life and provide a new understanding of how microorganisms may enhance industrial processes, particularly in nanotechnology production. In 1926, Bastin discovered sulfur-reducing bacteria such as *Desulfoplanes*, *Desulfovermiculus*, and *Desulfotignum* within harsh environments (Kadnikov et al. 2023). The study of microbial communities in oil reservoir environments has since opened a new chapter in our understanding of these ecosystems, subsequent research has revealed diverse microorganisms inhabiting oil reservoirs, including those found in crude oil, formation water, rocks, and organic matter, particularly in the oil-to-water transition zone (OWTZ), conducive to microbial growth and oil decomposition (Rajbongshi & Gogoi 2021). The positive effects of these microbial communities can be harnessed by investigating their activities, metabolic processes, and capacity to produce bio-products such as surfactants, biopolymers, solvents, acids, and gases (Augustine 2023). Much current research focuses on oil contaminated environments, where *Alishewanella jeotgali*, *Bacillus cereus* and *Pseudomonas stutzeri* have likely adapted to harsh conditions and developed significant enzyme systems of interest for both environmental and commercial applications (AL-assdy et al. 2024; AL-Shami et al. 2023; Alyousif et al. 2022; Aboud et al. 2021; Hamzah et al. 2020 a). Among these applications, the biosynthesis of AgNPs is gaining attention due to its environmentally friendly, energy-efficient, cost-effective, and rapid nature compared to traditional physical and chemical methods (Yali et al., 2023). Furthermore, AgNPs have diverse applications in medicine, food technology and environmental science (Arshad et al., 2024). The degradation of mixture polluted compounds like oil spills, heavy metals, herbicides, particulate matter, pesticides, fertilizers, toxic gases, sewage and industrial effluents (Singh et al., 2020), can be done professionally with the help of nanocatalyst (Astruc, 2020). Recent studies indicate a direct relationship between nitrate reduction by microorganisms and their ability to synthesize AgNPs, evidence suggests that the biological reduction of nitrate may release free electrons, which can subsequently reduce silver ions ( $\text{Ag}^+$ ) to form AgNPs, this mechanism highlights the bacteria's capacity to transform toxic metals into non-toxic nano forms and produces AgNPs with unique properties (Rose et al., 2023). The connection between nitrate reduction and nanoparticle synthesis underscores the importance of studying this process to understand better the biological mechanisms involved in the biosynthesis of AgNPs. The nanoparticles can be produced by extracellular or intracellular by bacteria, often involving organic molecules such as proteins, sugars, and enzymes, these are believed to be crucial in reducing metal ions and forming nanoparticles through oxidation-reduction reactions (John et al., 2022). Despite the significant advancements in nanoparticle biosynthesis, gaps remain in our understanding of how microorganisms convert metals into nanoparticles, especially in oilfield environments (Bharose et al., 2024). Characterizing the bacterial community structure of the produced waters from oil fields faces significant challenges, including the difficulty of bacteria using conventional methods, does not rely solely on cultural methods but rather on molecular methods of analysis (Ziganshina et al., 2023). Therefore, DNA sequencing approaches particularly

the gene of *16SrDNA* have greatly enhanced our understanding of these microbial communities and their compositions (Gao et al., 2024). Research has revealed a remarkable diversity of bacterial species inhabiting oil reservoirs, with hundreds recorded and several species identified for their high capacity to produce AgNPs, paving the way for new insights in biological research and nanotechnology. In Badra and Ahdab oil fields, the existing of bacterial community have not yet been explored, and there is no data available. Hence, the present study aims to isolate and identify bacteria from the reservoirs of these oil fields in Wasit Governorate, Iraq, and determine the most efficient isolates for synthesized AgNPs with characterizing the produced nanoparticles by different ways.

## 2. MATERIALS AND METHODS

### 2.1. Sample collection

Eight samples of produced water were collected from separator tanks of the Badra and Ahdab oil fields between October and December 2022. The Badra oil field is located at the northeast of Wasit Governorate in Iraq at approximately  $33.037^{\circ}\text{N}$  and  $46.056^{\circ}\text{E}$ . The depth of oil reservoirs was between 4700 and 6200 m below ground, depending on primary production of oil, while in the Ahdab oil field, located to the west of Wasit at approximately  $32.424^{\circ}\text{N}$  and  $45.714^{\circ}\text{E}$ , the oil reservoirs were between 2300 and 3500 m deep, extracting oil through flooding with water for secondary production Fig. 1. The samples were collected in sterile glass containers and transported to the laboratory immediately; keep at room temperature until used. Daily reports from the oil field laboratories were used to determine the physical and chemical properties of the samples Table 1.

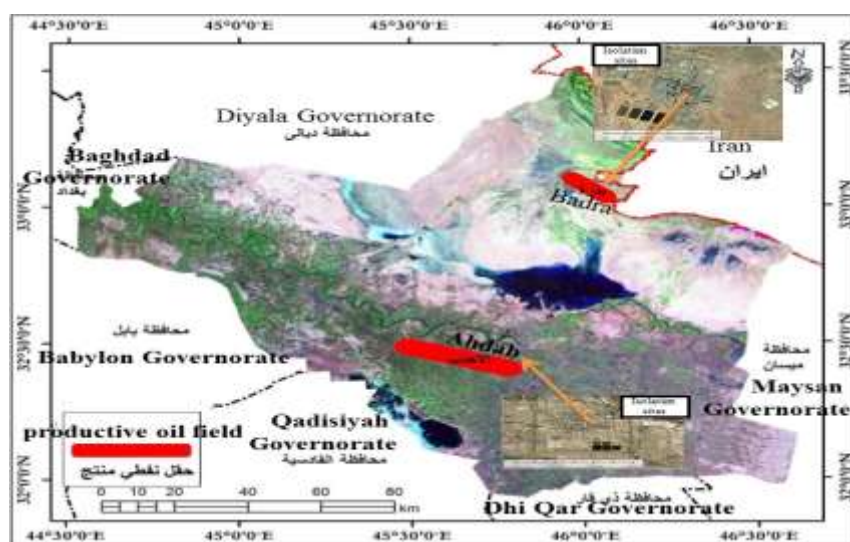


**Fig. 1:** Sample collection sites.

**Table 1:** physiochemical properties of the produced water samples obtained from Badra and Ahdab oil fields.

Samples	Oil in water ppm	TSS ppm	pH	Total Iron ppm	Hydrogen sul- fide ppm	Chloride ppm
BD- s 1	85	20.0	6.6	0.69	371.96	21423
BD- s 2	92	15.0	6.8	0.78	400	19080
Ah- s1	36.94	37.0	6.85	0.10	406	130804.81
Ah- s2	34.15	42.0	6.87	0.10	377	143362.65

BD= Badra, Ah=Ahdab, s= sites, TSS= Total Suspended Solids

## 2.2. Culturing of Bacteria

To isolate the indigenous bacteria, 5mL of each sample was inoculated into a 250mL Erlenmeyer flask containing 95 mL of nutrient broth. The flasks were incubated in a shaker at 35°C and 120 rpm for 48 hrs. After the incubation period, 1 ml from each flask was serially diluted and spread using an L-shaped glass spreader onto the center of sterilized nutrient agar and MacConkey agar plates and incubated aerobically at 35°C for 24hrs. Distinct colonies were isolated, and the subculture process was conducted three times to ensure the purity of the colonies. Additionally, the Gram stain protocol was employed for microscopic analysis.

## 2.3. Molecular Identification of Bacteria

Each isolate was activated for 24 hours at 35°C in nutrient broth medium. An Eppendorf tube containing 1.5 ml of culture was centrifuged for two minutes at 13,000 rpm. After discarding the supernatant, DNA was extracted from the cells by the Presto™ Mini gDNA kit according to the manufacturer's instructions (Geneaid, Taiwan). A 1% agarose gel was used to prove the extracted gene's existence. Identification of the isolated bacteria was performed using a 1500-bp-long *16SrDNA* gene. Polymerase chain reaction (PCR) was used for amplification, using the universal forward primer 27F 5'-AGAGTTTGATCCTGGCTCAG-3' and the reverse primer 1492R 5'GGTTACCTTGTACGACTTR-3'. The AccuPower® PCR PreMix kit prepared the reaction mixture according to the manufacturer's instructions. The program of the thermal cycle was as follows: initial denaturation at 95°C for 5min., followed by denaturation with 30 cycles of 95°C for 30 sec., primer annealing at 52°C for 45sec., extension at 72°C for 1.5min., and final extension at 72°C for 10min. (Alyousif et al., 2020). To verify the amplification of the target gene, the fragment of amplified DNA was separated using an electrophoresis device on a 1.5% (w/v) agarose gel stained with 0.5 µl of ethidium bromide to a concentration of 0.5 µg/ml (Lee et al., 2012). The amplified and labeled DNA tubes were sent to Macrogen Laboratories in South Korea for sequence analysis. The results were compared with the NCBI website using BLAST to identify the closest matches to the bacterial isolate. The phylogenetic tree was constructed using the neighbor-joining (NJ) technique in MEGA 11, with 1000 primers incorporated to ensure robustness (Burghal et al. 2021).

## 2.4. Screening the Ability of Bacterial Isolates for Synthesize AgNPs

All bacterial isolates were screened for the synthesis of AgNPs by the nitrate reduction test which conducted according to Bhusal & Muriana (2021). The positive isolates were selected for screened on nutrient agar supplemented with 1 mM AgNO<sub>3</sub>, the bacterial isolates were inoculated on the plates, incubated at 35°C for 24 to 72 hrs. The growth of bacteria indicated a positive result, the isolates that gave positive result were choices for the final screening which carried out to select the most efficient isolates for synthesized AgNPs, based on changes in the color of the reaction mixture, following the method described by Bhusal & Muriana (2021) with some modifications. Selected bacterial strains were cultured in 250 ml Erlenmeyer flask, incubated in a shaker at 35°C with a speed of 180 rpm for 24 hrs. After incubation, the cultures were centrifuged at 6000 rpm for 20 min. The resulting supernatant was then filtered using a Millipore filter with a pore diameter of 0.45 µm. Next, the reaction mixture was prepared by mixing equal volumes 1:1 (v/v) of the supernatant and a 1mM AgNO<sub>3</sub> solution in an aluminum-coated flask to prevent oxidation. The mixture was then incubated in a shaker at 180 rpm and 35°C for 72 to 120 hrs. The results were evaluated by observing the color change of the reaction mixture from yellow to dark brown compare with control (nutrient broth with AgNO<sub>3</sub> solution). After the incubation period, to confirm the presence of AgNPs in the reaction mixture, 2ml of each mixture that changed color to brown was taken and poured into a quartz cuvette. The absorbance was measured in the range of (200-800) nm using the UV-1800 double-beam spectrophotometer (Shimadzu, Japan).

## 2.5. Purification of AgNPs

After measuring the absorbance, the reaction mixture that achieved the highest absorbance peak was placed in test tubes in a centrifuge at 6000 rpm for 20 minutes, the supernatant was discarded, and the remaining precipitate was washed with deionized distilled water. This step was repeated thrice until a clear and colorless solution was obtained. In the final step of centrifugation, the precipitate containing AgNPs was placed in a clean watch glass in an electric oven at 50°C to dry and remove excess water. The resulting powder was then collected in Eppendorf tubes covered with aluminum foil (AL-Shami et al. 2023).

## 2.6. Characterization of AgNPs Synthesized

The *Bacillus halotolerans* strain AhWM4 that gave the highest peak in the UV-visible spectrophotometer was characterized by an infrared spectrometer (Shimadzu, Japan). An X-ray diffractometer (PANalytical, Netherlands) is employed to ascertain the crystalline characteristics of AgNPs and to compute their size utilizing the Debye-Scherrer equation (Saleh & Alwan, 2020). The detailed structure of the AgNPs was studied using a field emission scanning electron microscope (FE-SEM) and transmission electron microscope (TEM) (Hitachi, Japan), while the elemental composition was determined with energy dispersive X-ray spectroscopy (EDX). A zeta potential device (HORIBA Scientific SZ-100, Japan) was used to assess the surface charges of AgNPs, and

dynamic light scattering (DLS) was employed to analyze the particle size and distribution in the colloidal solutions (Pallavi et al. 2022).

### 3. RESULTS

#### 3.1. Isolation of Bacteria

Twenty-five strains were isolated from produced water of the Badra and Ahdab oil fields. 15 (60%) isolates from the Badra oil field and 10 (40%) from Ahdab. According to the protocol of Gram stain. In the Badra oil field, 4 (26.7%) isolates were Gram negative and 11 (73.3%) were Gram positive, while in Ahdab, the numbers of Gram negative and positive isolates were 3 (30%) and 7 (70%), respectively as Fig. 2.

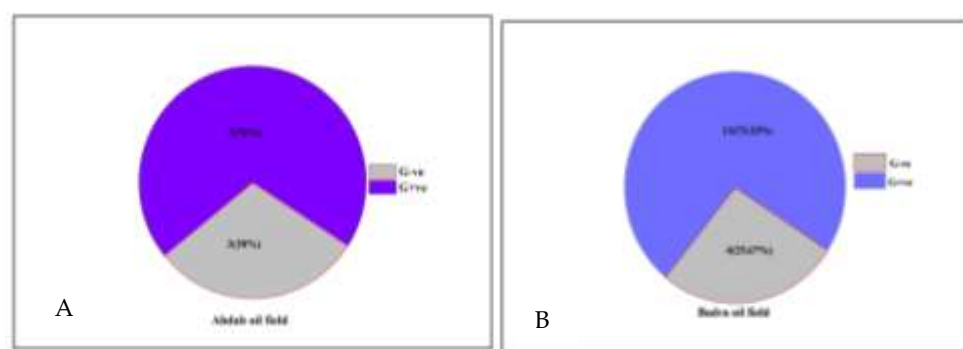


**Fig. 2:** Total percentage of Gram-positive and Gram-negative bacteria in produced water samples, A Ahdab oil field and B Badra oil field.

#### 3.2. Genetic Identification of Bacterial Isolates

The *16S rDNA* gene was amplified in order to identify the bacterial isolates using the polymerase chain reaction (PCR) technique. Agarose gels 1% (w/v) displaying PCR-amplified 16S rDNA gene fragments utilizing. About 1,500 bp of amplified fragments were obtained for every isolate, determined based on the DNA marker (100 bp) Fig. 3.

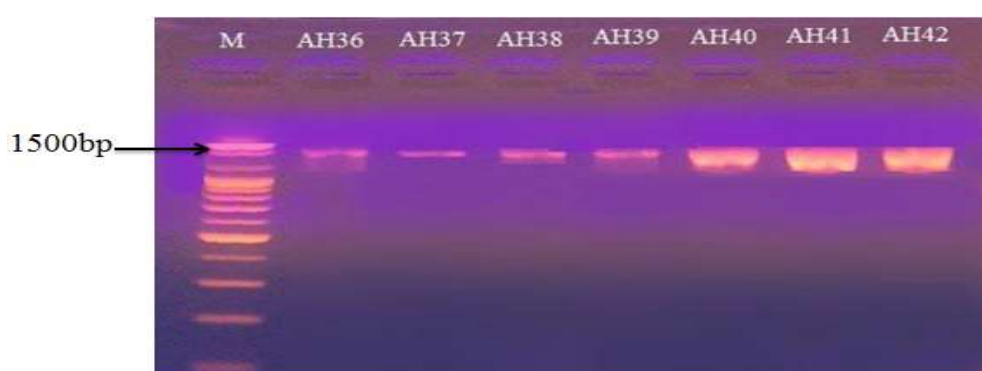


**Fig. 3:** Electrophoretic analysis demonstrating the amplified *16S rDNA* gene products derived from genomic DNA of some bacterial isolates. M. Ladder, AH36-AH42 AH code of bacterial isolates.

The BLAST tool was used to analyze and compare the DNA sequencing results of the bacterial isolates with those of the reference strains found in the GenBank database. The DNA sequencing results of most of the studied strains showed a 100% similarity in gene sequences compared to the reference strains as in Table 2. However, some isolated strains displayed variations in certain nitrogenous bases relative to the reference strains available in GenBank. Seven new strains were recorded in the GenBank database, with unique accession numbers as illustrated in Table 3.

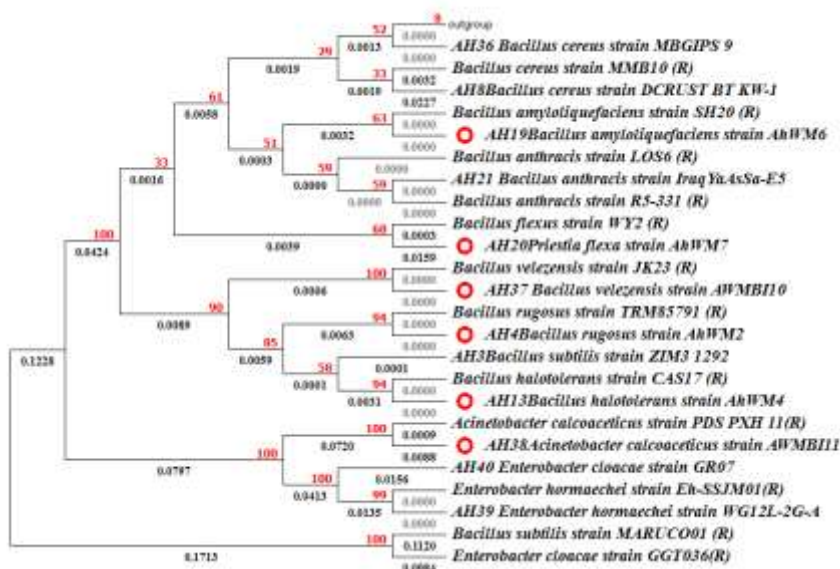
**Table 2:** Bacterial community of produced water samples that were identified by the *16S rDNA* gene (Ah= Isolation symbol before molecular identification, BD= Badra oil field, Ah= Ahdab oil field).

Site	Isolates code	Accession no. reference strain	Cloest species	Match ratio with reference strain %
BD- s1	AH42	OM033656.1	<i>Enterobacter hormaechei</i>	100 %
	AH45	MN208152.1	<i>Enterobacter cloacae</i>	100 %
	AH14	OP852942.1	<i>Bacillus paramycooides</i>	98 %
	AH38	MN049561.1	<i>Acinetobacter calcoaceticus</i>	99 %
	AH36	KX950679.1	<i>Bacillus cereus</i> strain MBGIPS 9	100 %
	AH37	MN847602.1	<i>Bacillus velezensis</i>	99 %
	AH31	KF051091.1	<i>Flavobacterium columnare</i>	100 %
BD- s2	AH18	FJ573187.1	<i>Bacillus cereus</i> strain AK1871	100 %
	AH46	MT000148.1	<i>Enterococcus faecium</i>	100 %
	AH19	KY362201.1	<i>Bacillus amyloliquefaciens</i>	99 %
	AH30	KC790242.1	<i>Bacillus anthracis</i>	100 %
	AH11	MK547152.1	<i>Bacillus tropicus</i>	100 %
	AH10	MZ618716.1	<i>Bacillus subtilis</i>	100 %
	AH21	ON510000.1	<i>Bacillus anthracis</i>	100 %
Ah- s1	AH20	KR999903.1	<i>Priestia flexa</i>	99 %
	AH47	MN658825.1	<i>Enterobacter hormaechei</i>	100 %
	AH39	OP288194.1	<i>Enterobacter hormaechei</i>	100 %
	AH41	MT783973.1	<i>Bacillus cereus</i>	100 %
	AH40	MH050744.1	<i>Enterobacter cloacae</i>	100 %
Ah- s2	AH4	OK298998.1	<i>Bacillus rugosus</i>	99 %
	AH5	OQ152470.1	<i>Bacillus toyonensis</i>	100 %
	AH15	KX268482.1	<i>Bacillus cereus</i>	100 %
	AH3	MT539995.1	<i>Bacillus subtilis</i>	100 %
	AH12	LK392517.1	<i>Bacillus cereus</i> strain ISU-02	100 %
	AH13	MT539148.1	<i>Bacillus halotolerans</i>	99 %

**Table 3:** The new bacterial strains that were deposited in NCBI GenBank database

Name of the new strain in GenBank	Accession no.
<i>Bacillus paramycoïdes</i> strain AhWM5	PP559174.1
<i>Acinetobacter calcoaceticus</i> strain AWMBI11	PP564426.1
<i>Bacillus velezensis</i> strain AWMBI10	PP564424.1
<i>Bacillus amyloliquefaciens</i> strain AhWM6	PP559314.1
<i>Priestia flexa</i> strain AhWM7	PP559502.1
<i>Bacillus rugosus</i> strain AhWM2	PP558901.1
<i>Bacillus halotolerans</i> strain AhWM4	PP559020.1

The results of the phylogenetic tree also confirmed a clear genetic proximity between the studied isolates and the reference strains as shown in Fig. 4.

**Fig. 4:** A phylogenetic tree that shows the evolutionary relationships among bacterial strains of different species and their reference strains (R).

DNA sequencing of the bacterial community of produced water samples revealed that bacterial isolates were under six different bacterial genera and belonged to sixteen species. The genera were *Enterococcus*, *Priestia*, *Enterobacter*, *Acinetobacter*, *Flavobacterium*, and *Bacillus*. Among them, the genus *Bacillus* was the most prevalent, 16 (64%), followed by *Enterobacter*, 5 (20%). For the species, *Bacillus cereus* was the most frequently recorded, 5 (20%), followed by *Enterobacter hormaechei*, 3 (12%) Fig. 5.

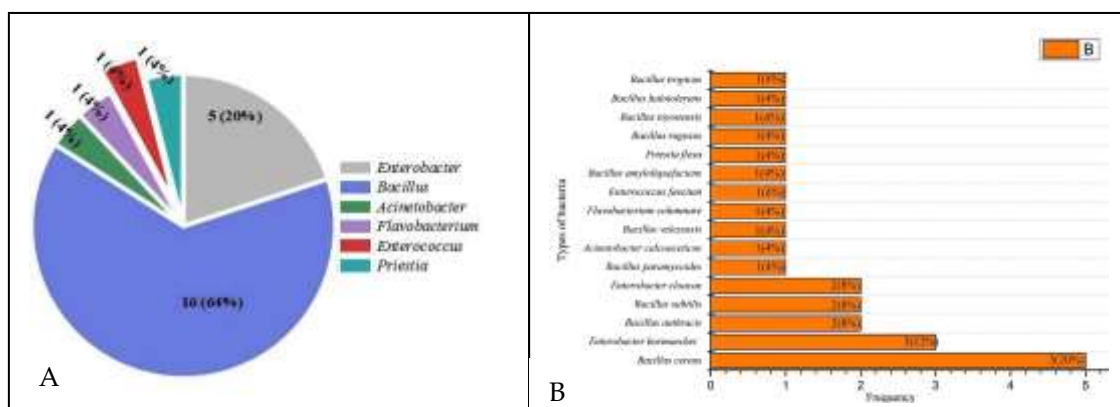


**Fig. 5:** Frequency of bacterial isolates in samples. (A). Percentage of genera (B). Percentage of species.

### 3.3. Screening of Bacterial Isolates for the Ability to Synthesize AgNPs

All bacterial isolates were tested for synthesis of AgNPs. The screening results by nitrate reductase enzyme test showed that 18 of the isolates gave positive results. Only these isolates were screened on nutrient agar supplemented with 1mM AgNO<sub>3</sub>, and the results revealed that only 11 showed growth. These isolates were tested for a color change, as the supernatant of bacterial cultures treated with 1 mM AgNO<sub>3</sub>. Only 2 strains, *Bacillus halotolerans* strain AhWM4 and *Bacillus rugosus* strain AhWM2, showed extracellular formation of AgNPs, which was initially validated by observing the color change of the supernatants from light yellow to brown compared to the control after the incubation period, indicating the formation of AgNPs Fig. 6.



**Fig. 6:** Screening of bacterial isolates based on color change of the mixture: (AH). Isolates. (C). Control.

The UV-vis spectrophotometer was used to detect the biosynthesis of AgNPs after the color change of the mixture reaction of two strains, AH 13 and AH 4. *Bacillus halotolerans* strain AhWM4 and *Bacillus rugosus* strain AhWM2. The results indicated a maximum absorption peak of 0.47  $\lambda_{\text{max}}$  at 430 nm and 0.09  $\lambda_{\text{max}}$  at a wavelength of 440 nm, using the supernatant for both strains, respectively, indicating the synthesis of AgNPs with different optical properties Fig. 7.

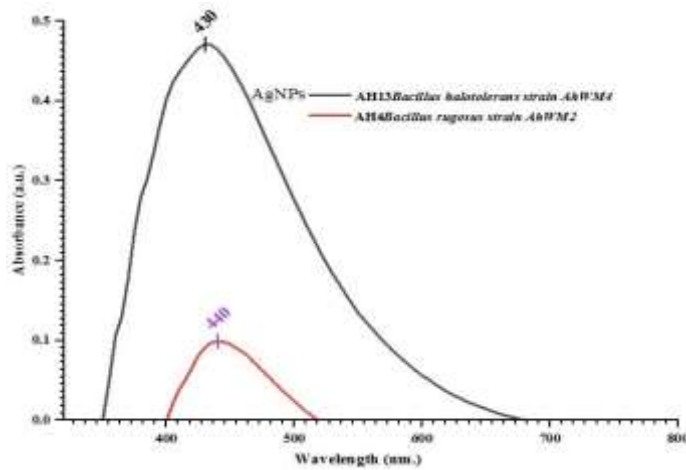


**Fig. 7:** UV-vis spectra of AgNPs biosynthesized by bacterial strains after color change in the reaction mixture.

### 3.4. Characterization of AgNPs synthesized by *Bacillus halotolerans* strain AhWM4

#### 3.4.1. Fourier Transform Infrared Spectroscopy (FTIR)

The FTIR spectra were used to identify the various functional groups of the synthesized AgNPs by *Bacillus halotolerans* strain AhWM4 that contributed to stability and the reduction of precursors to NPs. The results displayed peaks at specific wavelengths, specifically around 13495, 12935, and 1552  $\text{cm}^{-1}$ . These peaks correspond to O-H stretching from hydrogen-bonded alcohols and phenolic vibrations, as well as C-H bonds in alkanes and C=O bonds in carbonaceous compounds, ketones, aldehydes, and carboxylic acids. N-H bonds in amides and secondary amines. The results further indicated a shift and a decrease in the intensity of some bands in the spectrum of the AgNPs formed during the reduction process. Notably, the peaks at 3214.19  $\text{cm}^{-1}$ , 1647.21  $\text{cm}^{-1}$ , and 1554.86  $\text{cm}^{-1}$  showed a decrease in intensity and a shift in position Fig. 8.

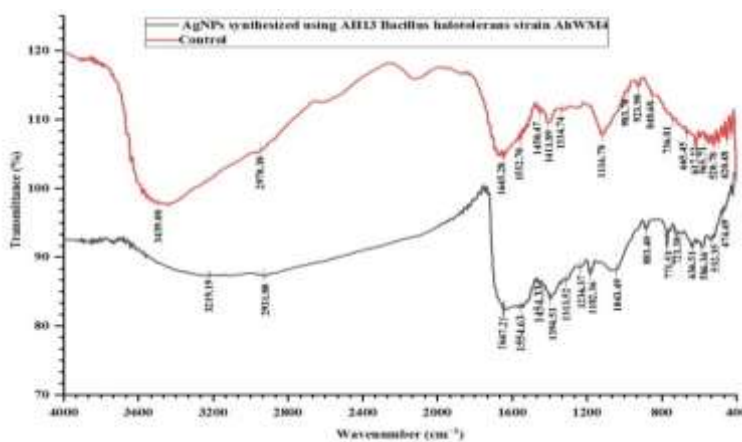


**Fig. 8:** FTIR spectra of control and Ag NPs synthesized by *B. halotolerans* strain AhWM4.

#### 3.4.2. The X-ray Diffraction (XRD) Analysis

The crystallinity of AgNPs synthesized by the *B. halotolerans* strain AhWM4 was examined using XRD analyses. Five distinct diffraction peaks were observed at  $2\theta$  values of  $38.27^\circ$ ,  $45.94^\circ$ ,  $55.59^\circ$ ,  $67.42^\circ$ , and  $76.94^\circ$ . These peaks correspond to the silver crystal planes (200, 103, 006, 112, and 201), closely matching the previously cited reference (JCPDS: 00-041-1402). Additionally, the X-ray diffraction (XRD) pattern exhibited three extra peaks at  $2\theta$  values of  $27.83^\circ$ ,  $32.32^\circ$ , and  $57.61^\circ$ , which could be associated with the crude coating agents Fig. 9. According to Scherrer's the average crystallite size of the AgNPs was calculated to be 31.3 nm.

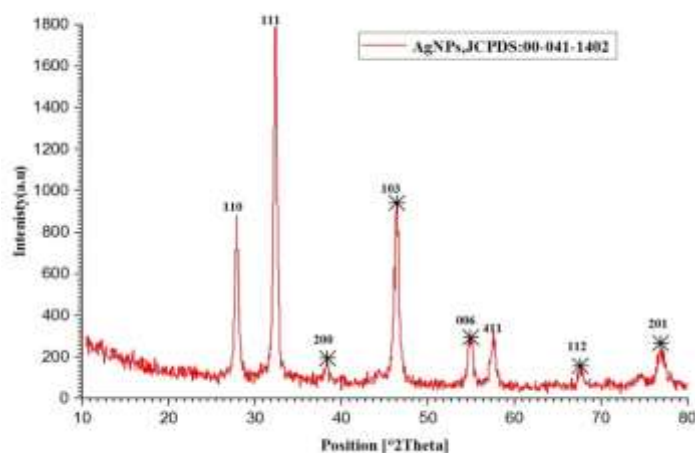


**Fig. 9:** XRD spectra of AgNPs synthesized by *B. halotolerans* strain AhWM4.

### 3.4.3. Electron Microscopy (FE-SEM)

According to the Field Emission Scanning Electron Microscopy (FE-SEM) and Transmission Electron Microscopy (TEM) images, the synthesized by the *B. halotolerans* strain AhWM4 were spherical or sub-spherical and exhibit a polydisperse nature. The average sizes of the nanoparticles were between 27.0 nm and 42.1 nm, respectively, with no signs of agglomeration Fig. 10.

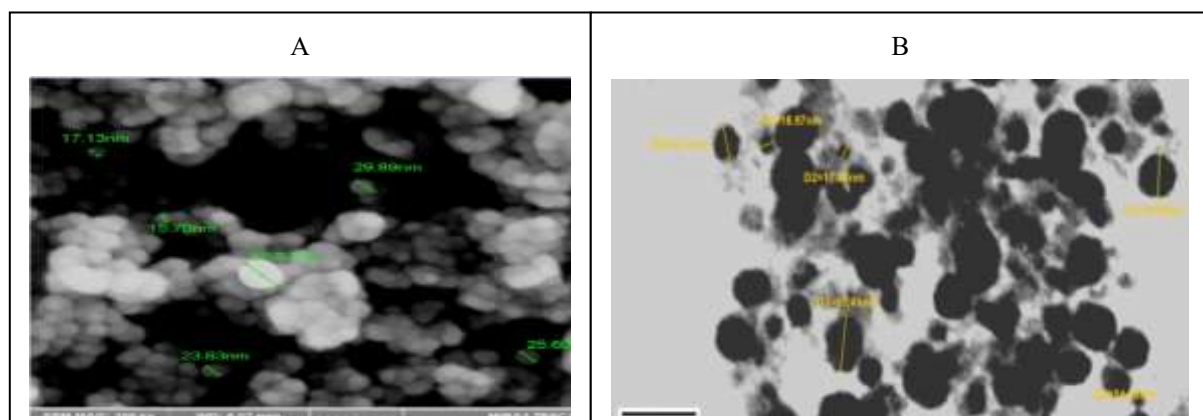


**Fig. 10:** Characteristic of AgNPs synthesized using *B. halotolerans* strain AhWM4: (A). FE-SEM (B). TEM.

### 3.4.4. Energy Dispersive X-Ray Spectroscopy (EDX) and Zeta Potential

The EDX analysis revealed that the elemental composition of the nanoparticles showed a significant peak at 3.0 keV, corresponding to an atomic percentage of 63.2%, indicating silver as the primary element. Additional peaks for carbon (C), oxygen (O), gold (Au), and nitrogen (N) are also observed throughout the scanning range (0–3 keV). Still, these elements are present at very low atomic percentages Fig.11. Zeta potential analysis was conducted to evaluate the electrostatic stability of the synthesized AgNPs. The zeta potential of AgNPs was measured at -42.3 mV, indicating their superior stability Fig.11.

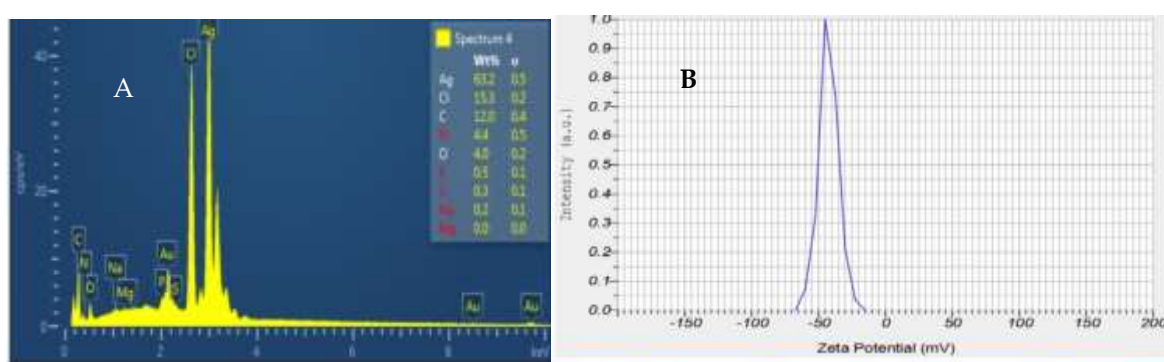


**Fig. 11:** Characteristics of AgNPs synthesized using *B. halotolerans* strain AhWM4. (A). EDX analysis. (B). Zeta potential value.

### 3.4.5. Dynamic Light Scattering (DLS)

Dynamic light scattering (DLS) was employed to assess the nanoparticles' hydrodynamic diameter and aggregation in colloidal solutions. The average diameter was found to be 123 nm; most of the synthesized AgNPs had an effective diameter of 57.1 nm and a polydispersity index (PI) of 0.52 Fig. 12.

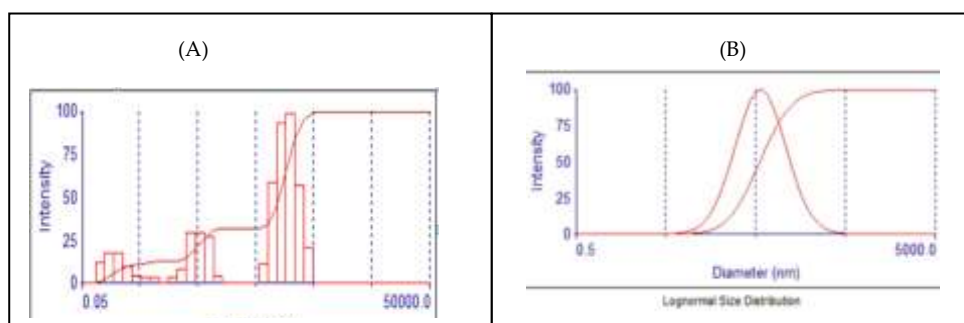


**Fig. 12.** Characteristic of AgNPs synthesized using *B. halotolerans* strain AhWM4 through (A). Lognormal Distribution Multimodal Size Distribution (B). Multimodal Size Distribution.

## 4. DISCUSSION

The current study demonstrated a remarkable diversity of bacterial species in produced water in the Badra and Ahdab oil fields. The number of bacterial isolates in the Badra oil field was higher than in Ahdab; this may be due to the differences in the physical and chemical properties of the two fields, Table 1. Other factors such as geographical location, age of the oilfield, depth, and method of oil production may also contribute (Alshami et al., 2022) reported that in oil reservoir environments, there was a great diversity of bacterial communities, influenced by a number of factors, despite their harsh environmental conditions.

The results showed that the number of Gram-positive isolates in both fields was higher than Gram-negative. This is consistent with the study of Vitaly et al. (2023). The Gram-positive bacteria have a thick peptidoglycan wall, spores, enzymes, and metabolic pathways that enable them to degrade the complex hydrocarbons present in oil and use them as an energy source, giving them additional protection and a high ability to withstand the harsh conditions (Huang et al. 2023). All bacterial isolates showed successful amplification of the 16SrDNA gene with fragments that were approximately 1,500 bp; these results were compatible with previous studies (AL-Salami et al. 2024; AL-Zaidi et al. 2023; Hamzah et al. 2020b). The current study showed a clear dominance of the genus *Bacillus*; this was consistent with previous studies (Alyousif et al. 2020; Al-Tamimi et al. 2019). *Bacillus* is known for its ability to adapt to harsh conditions. Its cell wall is composed of peptidoglycan compounds, teichoic acid, and meso-diaminopimelic acid, which enhance its rigidity. Endospores play a crucial role in the presence of this genus in these environments (Blanco Crivelli et al. 2024). These bacteria possess specific metabolic pathways that enable them to produce substances that inhibit other bacteria, giving them a competitive advantage in their living environment and making them a dominant genus in hydrocarbon-contaminated environments (Aboud et al. 2021). Through the sequencing of the 16SrDNA gene, seven unique bacterial strains for the current investigation have been registered in the NCBI GenBank database with particular accession codes. These bacterial isolates' DNA sequences may alter as a result of exposure to mutants; the cause of the mutation may be attributed to the difference in the ecological systems and exposure to mutagens, including chemicals and radiation. Several new bacterial strains isolated from Iraqi oil field environments have been reported (AL-assdy et al. 2025; Al Shami et al., 2022; Alyousif et al. 2020).

In the present study, all bacterial isolates from produced water of oil fields were screened for the synthesis of AgNPs. The bacterial isolates gave positive results for the nitrate reduction test and the ability to grow in the presence of 1 mM AgNO<sub>3</sub>. Nitrate can be converted to nitrite by NR enzyme, an NADH-dependent enzyme that takes up two electrons released by NADH oxidation. Released electrons can also reduce silver ions (Ag<sup>+</sup>) to AgNPs. Metal nanotization by microbes is an essential part of geo-cycles and happens as a response to the stress of heavy metals in harsh environments, resulting in an adaptive and protective mechanism for the microbe against the toxicity of metal (Ghosh et al. 2021). AgNPs were synthesized utilizing various methods, including bioreducing agents (Prodjosantoso et al., 2025). The results showed the ability of two bacterial isolate strains, *Bacillus halotolerans* strain AhWM4 and *Bacillus rugosus* strain AhWM2, to cause a color change of

the reaction mixture from light yellow to brown compared to the control. This change is an initial and visible indication of the production of AgNPs, which occurs due to surface plasmon resonance when they interact with light. Strain of *B. halotolerans* AhWM4 revealed a maximum absorption peak. Various factors, including the size and shape of the nanoparticles, influence the

differences in electron density within them. Smaller nanoparticles may exhibit a different color than larger ones due to the way they interact with light and the distribution of electrons within them, many previous studies have also indicated this (Alfryyan et al. 2022; Haji et al. 2022). UV-Vis, SEM, TEM, EDX, XRD, FTIR, zeta potential, and DLS were used to characterize biosynthesized AgNPs from the bacterial strain *B. halotolerans* AhWM4. The results of FTIR spectroscopy showed that bacterial supernatant contains compounds that can reduce Ag<sup>+</sup> ions and act as natural capping agents. Functional groups like ketones, aldehydes, carboxylic acids, and amides indicate a wide range of organic compounds, such as enzymes, proteins, amino acids, and carbohydrates, which may play a significant role in reducing silver ions and creating AgNPs. (Boldt et al. 2023; Al-Timimi et al. 2016). AgNPs have a consistent crystalline structure, as shown by XRD peaks, the pattern fits the JCPDS database standard pattern, demonstrating AgNP purity and hexagonal form (Lakhan et al., 2020). According to the Debye-Sherrer equation, the broad peaks indicate tiny particles with an average crystallographic size of 31.33 nm. The prominent peaks indicate that bacterial extract biomolecules stabilize AgNPs. These results are similar to previous studies (Ghiuta et al. 2021; Thirumagal & Jeyakumari, 2020).

The results are consistent with most previous research, which showed the spherical shape of AgNPs synthesized by different types of bacilli bacteria, as demonstrated by FE-SEM and TEM, with some differences in the size of the synthesized particles (Alsamhary 2020). These differences may be due to different factors, the concentration of metal ions, reaction mixture temperature, duration, and pH (Marooufpor et al. 2019). The AgNPs showed little agglomeration; this phenomenon can be attributed to biomolecules that play a crucial role in stabilizing the AgNPs and preventing their agglomeration (Khorrami et al. 2018). The EDX pattern showed a prominent silver peak with an atomic fraction of 63.2% at three keV, consistent with the standard location of silver associated with surface plasmon resonance (SPR). The EDX pattern showed peaks related to carbon, oxygen, and nitrogen. Low atomic ratios were detected in the spectrum's scanning range (0–3 keV). This indicates that a biological molecule, enzymes and proteins, was associated with the biosynthesis of AgNPs (Eid et al. 2024).

Zeta potential and DLS characterize nanoparticles precisely by the particle size and surface charge of AgNPs. Zeta potential tests were conducted to assess the colloidal stability of AgNPs, as illustrated in the result of 42.3 mV, which signifies high stability (Saied et al. 2024) Reported zeta potentials of -30, -34.1, -33.9, and -21.4 mV. Silver nanoparticles' negatively charged zeta potential induces electrostatic repulsion, stabilizing them

and inhibiting agglomeration (Solís-Sandí et al. 2023). The bacterial extract's carboxyl group (COOH) is responsible for the negative charge, as proven by FT-IR analysis (Illanes Tormena et al. 2024). DLS measures the hydrodynamic radius of nanoparticles, which is influenced by their size, the conjugated molecules, sugar, protein, and the random or Brownian motion in solution.

## 5. CONCLUSIONS

Numerous factors influence the high diversity of bacterial communities that are found in produced water oil fields, despite their extreme environmental circumstances. Gram-positive bacteria outnumbered Gram-negative in these environments. *Bacillus* spp. was the most prevalent, with the predominant species of *Bacillus cereus*. The novel strain of *B. halotolerans* AhWM4 was the most effective and powerful in synthesizing AgNPs with distinct properties, an average diameter within the nanoscale range, spherical shape, and high stability in aqueous solutions, which makes it eligible for use in many medical, pharmaceutical, and environmental applications for treating various types of pollutants in the water and soil environment.

**Funding:** This research received no external funding.

**Acknowledgments:** The Department of Biology at the College of Science, University of Basrah, Iraq, is to be greatly thanked by the authors for providing the necessary facilities that enabled this study.

**Conflicts of Interest:** "The authors declare no conflicts of interest." "The funders had no role in the design of the study; in the collection, analysis, or interpretation of data; in the writing of the manuscript; or in the decision to publish the results."

## REFERENCES

1. Aboud, E. M., Burghal, A., & Laftah, A. H. 2021. Genetic identification of hydrocarbons degrading bacteria isolated from oily sludge? and petroleum-contaminated soil in Basrah City, Iraq. *Biodiversitas Journal of Biological Diversity*, 22(4). <https://doi.org/10.13057/biodiv/d220441>.
2. AL-assdy, H.Q., Al-Tamimi, W.H. & Almansoory, A.F. 2024. Extracellular Synthesis of Iron Oxide NPs by Using Several Bacteria Genera Isolated from Oil Contaminated Sites in Basrah Governorate. *Egyptian Journal of Aquatic Biology & Fisheries.*, 28(4): 1895 – 1914. <https://doi.org/10.21608/ejabf.2024.375219>.
3. AL-assdy, H.Q., Al-Tamimi, W.H., & Almansoory, A.F. 2025. Molecular detection of bacteria isolated from polluted environment and screening their ability to produce extracellular biopolymer flocculants. *Beni-Suef Univ J Basic Appl Sci*, 14: 29. <https://doi.org/10.1186/s43088-025-00621-1>.
4. Alfryyan, N., Kordy, M.G.M., Abdel-Gabbar, M., et al. 2022. Characterization of the biosynthesized intracellular and extracellular plasmonic silver nanoparticles using *Bacillus cereus* and their catalytic reduction of methylene blue. *Sci. Rep.*, 12: 12495. <https://doi.org/10.1038/s41598-022-16029-1>
5. AL-Salami, R. B., Mukhaifi, E. A., & AL-Tamimi, W. H. 2024. Investigation of the effect of electric field on bacteria isolated from skin infection. *Biodiversitas Journal of Biological Diversity*, 25(3). <https://doi.org/10.13057/biodiv/d250348>.

6. Alsamhary, K.I. 2020. Eco-friendly synthesis of silver nanoparticles by *Bacillus subtilis* and their antibacterial activity. *Saudi J. Biol. Sci.*, 27(8): 2185-2191.2 <https://doi.org/10.1016/j.sjbs.2020.04.026>.
7. AL-shami, H. G. A., Al-Tamimi, W. H., & Hateet, R. R. 2022. Screening for extracellular synthesis of silver nanoparticles by bacteria isolated from Al-Halfaya oil35 field reservoirs in Missan36 province, Iraq. *Biodiversitas Journal of Biological Diversity*, 23(7). <https://doi.org/10.13057/biodiv/d230720>
8. AL-shami, H. G. A., Al-Tamimi, W. H., & Hateet, R. R. 2023. The antioxidant potential of37 copper oxide nanoparticles synthesized from a new bacterial strain. *Biodiversitas Journal of Biological Diversity*, 24(5). <https://doi.org/10.13057/biodiv/d240519>.
9. Al-tamimi, W. H., Lazim, S. A., Abd Al-sahib, M. A., Hameed, Z. M., Al-amara, S. S. M., Burghal, A. A., & Al-maqtoofi, M. Y. 2019. Improved oil recovery by using biosurfactants produced from bacilli bacteria isolated from oil reservoirs in Iraq. *Poll. Res*, 38: 551-556. <https://www.researchgate.net/publication>.
10. Al-Tamimi, W.H., Lazim, S.A., Abd Al-sahib, M.A., Hameed, Z.M., Al-Amara, S.S.M., Burghal, A.A., & Al-Maqtoofi, M.Y. 2019. Improved oil recovery by using biosurfactants5 produced from bacilli bacteria isolated from oil reservoirs in Iraq. *Pollut. Res.*, 38: 551-556.
11. Al-Timimi, I.A.J., Sermon, P.A., Burghal, A.A., Salih, A.A., & Alrubaya, I.M. 2016. Nanoengineering the antibacterial activity of biosynthesized nanoparticles of TiO<sub>2</sub>, Ag, and Au and their nanohybrids with Portobello mushroom spore (PMS) (TiO<sub>x</sub>/PMS, Ag/PMS, and Au/PMS) and making them optically self-indicating. *Biosens. Nanomed.* IX, 9930: 42-54. SPIE. <https://doi.org/10.1117/12.2237643>
12. Alyousif, N. A., Al-Tamimi, W. H., & Abd Al-Sahib, M. A. 2022. Evaluation of the effect of various nutritional and environmental factors on biosurfactant production by *Staphylococcus epidermidis*. *Biodiversitas Journal of Biological Diversity*, 23(7): 3533-3538. <https://doi.org/10.13057/biodiv/d230729>.
13. Alyousif, N., Al Luabi, Y. Y., & Hussein, W. 2020. Distribution and molecular characterization of biosurfactant-producing bacteria. *Biodiversitas Journal of Biological Diversity*, 21(9): 4034-4040. <https://doi.org/10.13057/biodiv/d210914>.
14. AL-Zaidi, M. H.41 H., AL-Tamimi, W. H., & Saleh, A. A. A. 2023. Molecular determination of the microbial diversity associated with vaginitis and testing their sensitivity to selected antimicrobials. *Biodiversitas Journal of Biological Diversity*, 24(8): 4253-4261. <https://doi.org/10.13057/biodiv/d240806>.
15. Arshad, F., Naikoo, G.A., Hassan, I.U., et al. 2024. Bioinspired and green synthesis of silver nanoparticles for medical applications: A green perspective. *Appl. Biochem. Biotechnol.*, 196: 3636–3669. <https://doi.org/10.1007/s12010-023-04719-z>.
16. Astruc, D. 2020. Introduction: Nanoparticles in Catalysis. *Chemical reviews*, 120(2): 461–463. <https://doi.org/10.1021/acs.chemrev.8b00696>.
17. Augustine, J.A. 2023. Degradative potential of bacteria isolated from crude oil contaminated soil. *bioRxiv*, 2023: 10. <https://doi.org/10.1101/2023.10.16>.
18. Bharose, A.A., Hajare, S.T., G, H.P., Soni, M., Prajapati, K.K., Singh, S.C., & Upadhye, V. 2024. Bacteria-mediated green synthesis of silver nanoparticles and their antifungal potentials against *Aspergillus flavus*. *PLOS ONE*, 19(3): e0297870. <https://doi.org/10.1371/journal.pone.0297870>.

19. Bhusal, A., & Muriana, P.M. 2021. Isolation and characterization of nitrate-reducing bacteria for conversion of vegetable-derived nitrate to "natural9 nitrite". *Appl. Microbiol.*, 1(1): 11–23. <https://doi.org/10.3390/applmicrobiol1010002>.
20. Blanco Crivelli, X., Cundon, C., Bonino, M.P., Sanin, M.S., & Bentancor, A. 2024. The complex and changing genus *Bacillus*: A diverse bacterial powerhouse for many applications. *Bacteria*, 3(3): 256-270. <https://doi.org/10.3390/bacteria3030017>.
21. Boldt, A., Walter, J., Hofbauer, F., Stetter, K., Aubel, I., Bertau, M., Jäger, C.M., & Walther, T. 2023. Cell-free synthesis of silver nanoparticles in spent media of different *Aspergillus* species. *Eng. Life Sci.*, 23(3): e202200052. <https://doi.org/10.1002/elsc.202200052>.
22. Burghal, A.A., Al-Tamimi, W.H., & Al-Amara, S.S.M. 2021. A novel optimistic oil-degrading bacterium *Kocuria flava* Basra AWS strain. *Pollut. Res.*, 40: S200–S205.
23. Eid, A.M., Hassan, S.E.D., Hamza, M.F., Selim, S., Almuhayawi, M.S., Alruhaili, M.H., Tarabulsi, M.K., Nagshabandi, M.K., & Fouda, A. 2024. Photocatalytic, antimicrobial, and cytotoxic efficacy of biogenic silver nanoparticles fabricated by *Bacillus amyloliquefaciens*. *Catalysts*, 10 14(7): 419. <https://doi.org/10.3390/catal14070419>.
24. Gao, Y., Wang, W., Jiang, S., Jin, Z., Guo, M., Wang, M., Li, H., & Cui, K. 2024. Response characteristics of the community structure and metabolic genes of oil-recovery bacteria after targeted activation of petroleum hydrocarbon-degrading bacteria in low-permeability oil reservoirs. *ACS Omega*, 9(31): 33448–33458. <https://doi.org/10.1021/acsomega.3c10334>.
25. Ghiuta, I., Croitoru, C., Kost, J., Wenkert, R., Munteanu, D. 2021. Bacteria-mediated synthesis of silver and silver chloride nanoparticles and their antimicrobial activity. *Appl. Sci.*, 11(7): 3134. <https://doi.org/10.3390/app11073134>.
26. Ghosh, S., Ahmad, R., Banerjee, K., AlAjmi, M. F., & Rahman, S. 2021. Mechanistic aspects of microbe-mediated nanoparticle synthesis. *Frontiers in Microbiology*, 12: 638068. <https://doi.org/10.3389/fmicb.2021.638068>
27. Ziganshina, E. E., Mohammed, W. S., & Ziganshin, A. M. 2023. Microbial Diversity of the Produced Waters from the Oilfields in the Republic of Tatarstan (Russian Federation): Participation in Biocorrosion. *Applied Sciences*, 13(24), 12984. <https://doi.org/10.3390/app132412984>
28. Lee, P.Y., Costumbrado J., Hsu C.Y., Kim, Y.H. 2012. Agarose gel electrophoresis for the separation of DNA fragments. *J Vis Exp.* (62), e3923. <https://dx.doi.org/10.3791/3923>
29. Haji, S.H., Ali, F.A., & Aka, S.T.H. 2022. Synergistic antibacterial activity of silver nanoparticles biosynthesized by carbapenem-resistant Gram-negative bacilli. *Sci. Rep.*, 12: 15254. <https://doi.org/10.1038/s41598-022-19698-0>.
30. Hamzah, A., Abd-Alsahib, W., & Mahdi, S. 2020 b. Isolation and identification of new bacterial strains isolated from different sources of Al-Rafidiyah oil field in Iraq. Catrina: *Int. J. Environ. Sci.*, 21: 15–22. <https://doi.org/10.21608/cat.2020.23299.1041>.
31. Hamzah, A.F., Al-Mossawy,39 M.I., Al-Tamimi, W.H., et al. 2020a. Enhancing the spontaneous imbibition process using biosurfactants produced from bacteria isolated from Al-Rafidiya oil field for improved oil recovery. *J Petrol Explor Prod Technol.*, 10: 3767–3777. <https://doi.org/10.1007/s13202-020-00874-9.40>
32. Huang Y, Roseboom W, Brul S, Kramer G. 2023. Multi-omics analysis of *Bacillus subtilis* spores formed at different environmental temperatures reveals differences at the morphological and molecular level. *bioRxiv*. <https://doi.org/10.1101/2023.06.22.546136>.

33. Illanes Tormena, R.P., Medeiros Salviano Santos, M.K., Oliveira da Silva, A., Félix, F.M., Chaker, J.A., Freire, D.O., Rodrigues da Silva, I.C., Moya, S.E., & Sousa, M.H. 2024. Enhancing the antimicrobial activity of silver nanoparticles against pathogenic bacteria by using Pelargonium sidoides DC extract in microwave-assisted green synthesis. *RSC Adv.*, 14(30): 22035–22043. <https://doi.org/10.1039/d4ra04140b>.

34. John, M.S., Nagoth, J.A., Ramasamy, K.P., Mancini, A., Giuli, G., Miceli, C., & Pucciarelli, S. 2022. Synthesis of bioactive silver nanoparticles using new bacterial strains from an Antarctic consortium. *Mar. Drugs*, 20(9): 558. <https://doi.org/10.3390/md20090558>.

35. Kadnikov, V.V., Ravin, N.V., Sokolova, D.S., Semenova, E.M., Bidzheva, S.K., Beletsky, A.V., Ershov, A.P., Babich, T.L., Khisametdinov, M.R., Mardanov, A.V., et al. 2023. Metagenomic and culture-based analyses of microbial communities from petroleum reservoirs with high-salinity formation water, and their biotechnological potential. *Biology*, 12(10): 1300. <https://doi.org/10.3390/biology12101300>.

36. Khorrami, S., Zarrabi, A., Khaleghi, M., Danaei, M., & Mozafari, M.R. 2018. Selective cytotoxicity of green synthesized silver nanoparticles against the MCF-7 tumor cell line and their enhanced antioxidant and antimicrobial properties. *Int. J. Nanomedicine*, 13: 8013–8024. <https://doi.org/10.2147/IJN.S189295>.

37. Lakhan, M., Chen, R., Shar, A., Kumar, K., Chandio, M.B., Shah, A., Ahmed, M., Naich, R., & Wang, J. 2020. Illicium verum as a green source for the synthesis of silver nanoparticles and investigation of antidiatom activity against Paeodactylum tricornutum. *Sukkur IBA J. Emerg. Technol.*, 3: 23–30. <https://doi.org/10.30537/sjet.v3i1.495>.

38. Marououfpor, N., Alizadeh, M., Hatami, M., & Asgari Lajayer, B. 2019. Biological synthesis of nanoparticles by different groups of bacteria. In *R. Prasad* (Ed.), *Microbial nanobionics: Nanotechnology in the life sciences* 23 (pp. 1–20). Springer, Cham. [https://doi.org/10.1007/978-3-030-16383-9\\_3](https://doi.org/10.1007/978-3-030-16383-9_3).

39. Pallavi, S.S., Rudayni, H.A., Bepari, A., Niazi, S.K., & Nayaka, S. 2022. Green synthesis of silver nanoparticles using Streptomyces hirsutus strain SNPGA-8 and their characterization, antimicrobial activity, and anticancer activity against human lung carcinoma cell line A549. *Saudi J. Biol. Sci.*, 29(1): 228–238. <https://doi.org/10.1016/j.sjbs.2021.08.084>

40. Prodjosantoso, A.K., Nurul Hanifah, T.K., Utomo, M.P., Budimarwanti, C. and Sari, L.P., 2025. The Synthesis of AgNPs/SAC Using Banana Frond Extract as a Bioreducing Agent and its Application as Photocatalyst in Methylene Blue Degradation. *Nature Environment & Pollution Technology*, 24(1). <https://doi.org/10.46488/NEPT.2025.v24i01.D1688>

41. Rajbongshi, A., & Gogoi, S.B. 2021. A review on anaerobic microorganisms isolated from oil reservoirs. *World Journal of Microbiology and Biotechnology*, 37(7), p.111. <https://doi.org/10.1007/s11274-021-03080-9>.

42. Rose, G.K., Thakur, B., Soni, R., & Soni, S.K. 2023. Biosynthesis of silver nanoparticles using nitrate reductase from *Aspergillus terreus* N4 and their potential use as a non-alcoholic disinfectant. *Journal of Biotechnology*, 373:49–62. <https://doi.org/10.1016/j.jbiotec.2023.07.002>.

43. Saied, E., Abdel-Maksoud, M.A., Alfuraydi, A.A., Kiani, B.H., Bassyouni, M., Al-Qabandi, O.A., Bougafa, F.H.E., Badawy, M.S.E.M., & Hashem, A.H. 2024. Endophytic *Aspergillus hiratsukae* mediated biosynthesis of silver nanoparticles and their antimicrobial and photocatalytic activities. *Frontiers in Microbiology*, 15:1345423. <https://doi.org/10.3389/fmicb.2024.1345423>.

44. Saleh, M.N., & Alwan, S.K. 2020. Biosynthesis of silver nanoparticles from bacteria *Klebsiella pneumoniae*: Their characterization and antibacterial studies. *Journal of Physics: Conference Series*, 1664(1):1–15. <https://doi.org/10.1088/1742-6596/1664/1/012115>
45. Singh, J., Yadav, P., Pal, A., & Mishra, V. 2020. Water Pollutants: Origin and Status. In: *Sensors in Water Pollutants Monitoring: Role of Material*, pp. 5-20. Springer, Singapore. [https://doi.org/10.1007/978-981-15-0671-0\\_2](https://doi.org/10.1007/978-981-15-0671-0_2).
46. Solís-Sandí, I., Cordero-Fuentes, S., Pereira-Reyes, R., Vega-Baudrit, J.R., Batista-Menezes, D., & Montes de Oca-Vásquez, G. 2023. Optimization of the biosynthesis of silver nanoparticles using bacterial extracts and their antimicrobial potential. *Biotechnology Reports*, 40:e00816. <https://doi.org/10.1016/j.btre.2023.e00816>.
47. Thirumagal, N., & Jeyakumari, A.P. 2020. Structural, optical and antibacterial properties of green synthesized silver nanoparticles (AgNPs) using *Justicia adhatoda* L. leaf extract. *Journal of Cluster Science*, 31:487–497. <https://doi.org/10.1007/s10876-019-01663-z>.
48. Vitaly, V., Kadnikov, V.V., Ravin, N.V., Sokolova, D.S., Semenova, E.M., Bidzhieva, S.Kh., Beletsky, A.V., Ershov, A.P., Babich, T.L., Khisametdinov, M.R., Mardanov, A.V., & Nazina, T.N. 2023. Metagenomic and culture-based analyses of microbial communities from petroleum reservoirs with high-salinity formation water, and their biotechnological potential. *Biology*, 12. <https://doi.org/10.3390/biology12101300>.
49. Yali, R.R., Almansoory, A.F., & Al-Tamimi, W.H. 2023. Isolation and identification of bacteria from contamination by hydro-sites to produce AgNPs. *Marsh Bulletin*, 18(1). <https://faculty.uobasrah.edu.iq/uploads/publications/1701008349>.